Radical Cations of Branched Alkanes As Observed in Irradiated Solutions by the Method of Time-Resolved Magnetic Field Effect

V. I. Borovkov,*,†,‡ P. A. Potashov,†,‡ L. N. Shchegoleva,§ V. A. Bagryansky,† and Y. N. Molin†

Institute of Chemical Kinetics and Combustion of SB RAS, 3, ul. Institutskaya, Novosibirsk 630090, Russia, N. N. Vorozhtsov Institute of Organic Chemistry, 9, prosp. Akademika Lavrentyeva., Novosibirsk 630090, Russia, and Novosibirsk State University, 2, ul. Pirogova, Novosibirsk 630090, Russia

Received: March 7, 2007; In Final Form: May 7, 2007

Spin dynamics in radical ion pairs formed under ionizing irradiation of *n*-hexane solutions of two branched alkanes 2,3-dimethylbutane and 2,2,4-trimethylpentane has been studied by the method of time-resolved magnetic field effect in recombination fluorescence. Experimental curves of the magnetic field effect are satisfactorily described by assuming that the spin dynamics is determined by the hyperfine interactions in the radical cation (RC) of branched alkane under study with hyperfine coupling (HFC) constants averaged by internal rotations of RC fragments. The HFC constants determined from the magnetic field effect curves are close to those estimated within DFT B3LYP approach. Analysis of the results indicates that at room temperature the lifetimes of the RC of the studied branched alkanes amount to, at least, tens of nanoseconds.

I. Introduction

The radical cations (RCs) of aliphatic hydrocarbons have been studied in detail upon their stabilization in low-temperature matrices.[1−5] Under these conditions, it is possible to record both optical absorption and ESR spectra of these species as well as products of their decay. The advantage of ESR method is that it provides information on the structure of RC and its internal motions that lead to the modulation of hyperfine coupling (HFC) constants.

Less is known about RCs of alkanes formed in liquid solutions. The pulse radiolysis technique was used to observe absorption spectra of series of alkane RCs.[6,7] It was impossible, however, to apply a conventional ESR method under these conditions because of rather short lifetime of alkane RCs. Consequently, the ESR spectra of only a few alkane RCs have been detected using a highly sensitive method of optically detected ESR (OD ESR) of radical ion pairs.[8−11]

It was established that at room temperature the lifetime of the RC is within a submicrosecond range for some cyclic alkanes[8] and that falls into the range from several nanoseconds to several tens of nanoseconds for radical cations of *n*-alkanes.[10−12]

The data on the lifetimes of branched alkane RCs in liquid solutions are rather contradictory. On one hand, the OD ESR spectra of hexamethylethane RC has been detected in liquid *n*-pentane[10] and *n*-hexane,[13] thus indicating that the lifetime of this RC is, at least, several tens of nanoseconds. On the other hand, an opinion prevails that the RC of branched alkanes transform into some products over a subnanosecond time range. This view seems to be supported by the results reported by Tagawa et al. in ref 7. In the cited work the authors have attempted to observe the optical absorption of RCs of neopentane and 2,2,4-trimethylpentane at room temperature using the method of pulse radiolysis. However, no absorption bands that could be attributed to these RCs have been detected. Thus, the range of lifetimes of the radical cation of branched alkanes in solutions is still an open problem.

In this work, the method of time-resolved magnetic field effect (TR MFE) in recombination fluorescence of spin-correlated radical ion pairs[13−15] is applied to detect RCs of 2,3-dimethylbutane (DMB) and 2,2,4-trimethylpentane (TMP) in *n*-hexane solution at room temperature and to estimate the range of their lifetimes. In contrast to *n*-alkane RCs, which were investigated recently using the same approach,[16] RCs of branched alkanes being created in solution exhibited a resolved, partially, hyperfine structure. This allowed us to assign HFC constants with protons in these RCs, and to compare these with the results of the B3LYP/6-31G* calculations.

II. Experimental Section

The delayed fluorescence of *n*-hexane solutions of the studied branched alkane (+30 μM of *p*-terphenyl-d_{14}) was recorded using a nanosecond X-ray fluorometer described elsewhere.[17] A sample with a solution under study was irradiated by X-ray pulses with quantum energy of about 20 keV and a duration of about 2 ns. The fluorescence decays in the magnetic field of up to 1.15T and in zero field ($\pm$0.05 mT) were recorded in the single photon counting mode. OD ESR experiments were performed using the same setup as described elsewhere.[9,11]

n-Hexane and cyclohexane were treated with sulfuric acid, washed repeatedly with water, dried, and driven over Na. Then they were passed several times through a column with activated alumina. 2,3-Dimethylbutane (Fluka, 99%), 2,2,4-trimethylpentane (Fluka, 99%), and squalane (Aldrich, 99%) were passed through column with activated aluminum oxide. 2,4,4-Trimethylpentene-2 (98%), tetramethylethylene (98%), and *p*-terphenyl-d_{14} (98%) were used as received from Aldrich. Solutions were degassed by freeze−pump−thaw cycles. The experiments were performed within the temperature range of 253−323 K.

III. Theoretical Background of the Method of TR MFE

The time-resolved magnetic field effect (TR MFE) is usually determined as the ratio between the kinetics of recombination

* Corresponding author. E-mail: V. I. Borovkov, E-mail: borovkov@kinetics.nsc.ru.
† Institute of Chemical Kinetics and Combustion of SB RAS.
‡ Novosibirsk State University.
§ N. N. Vorozhtsov Institute of Organic Chemistry.

10.1021/jp071853h CCC: $37.00
Published on Web 06/13/2007

fluorescence $I(t)$ measured with and without magnetic field. For delayed fluorescence due to recombination of radical ion pairs we have[13−16]

$$\frac{I_B(t)}{I_0(t)} \approx \frac{\theta\rho_{ss}^B(t) + \frac{1}{4}(1-\theta)}{\theta\rho_{ss}^0(t) + \frac{1}{4}(1-\theta)} \quad (1)$$

Here θ is the portion of the pairs born in a singlet-correlated spin state, $\rho_{ss}(t)$ is the time-dependent population of the singlet spin state of the pairs, and the indices B and 0 correspond to the measurements made in high and zero magnetic fields, respectively. Evolution of the singlet state population $\rho_{ss}(t)$ in high and zero magnetic fields, respectively, obeys the equations[13,16]

$$\rho_{ss}^B(t) = \frac{1}{4} + \frac{1}{4}e^{-t/T_1} + \frac{1}{2}e^{-t/T_2}\cos\left(\frac{\Delta g\beta B}{\hbar}t\right)G_c^B(t)\,G_a^B(t) \quad (2)$$

$$\rho_{ss}^0(t) = \frac{1}{4} + \frac{3}{4}e^{-t/T_0}G_c^0(t)\,G_a^0(t) \quad (3)$$

where T_1 and T_2 are spin−lattice and phase relaxation times for electron spin polarization of radical pair in a high field, Δg is the difference in the g-factors of the radicals, T_0 is the effective time of the phase relaxation in zero field, and $G(t)$ is a function determined by HFC constants in radical ion. The indices a and c refer to radical anion and radical cation, respectively.

It is known that at high magnetic field, the $G^B(t)$ function can be expressed analytically upon arbitrary isotropic HFC constants in a radical. On the other hand, in zero magnetic field, an analytical formulation is possible only for a few cases, particularly for equivalent nuclei.[13] In the present work, except for tetramethylethylene RC, having 12 equivalent protons, $G_c^0(t)$ functions were calculated by means of a recently derived analytical solution for two groups of equivalent magnetic nuclei in a radical.[18] Expressions for these functions are rather cumbersome and can be found in the cited work. This approach is sure to be justified even if except for the two groups of magnetic nuclei having dominating HFC constants there are some nuclei with a smaller HFC in a radical. As shown in ref 19, the existence of small HFCs causes additional damping of oscillations in the TR MFE curves that looks like phase relaxation.

The contribution of *p*-terphenyl-d_{14} (*p*TP) radical anion to spin dynamics was calculated using a quasiclassical approximation[20] in terms of which $G_a^0(t)$ and $G^B(t)$ in eqs 2 and 3 are to be determined from the equations

$$G_a^0(t) = \frac{1}{3}[1 + 2(1 - \sigma^2t^2)\cdot e^{-\sigma^2t^2/2}] \quad (4)$$

$$G_a^B(t) = e^{-\sigma^2t^2/2} \quad (5)$$

where σ^2 is the second moment of radical anion ESR spectrum in units of angular frequency.

IV. Results of Quantum Chemical Calculations of Radical Cations Under Study

Conformations. Quantum chemical calculations of the stationary conformations and HFC constants of the RC under consideration were performed at the UB3LYP/6-31G* level using the GAMESS program.[21] We studied the adiabatic potential energy surface (PES) section along the rotation about the central C_2-C_3 bond in case of 2,3-dimethylbutane RC ($DMB^{+\bullet}$) and around the C_3-C_4 bond for 2,2,4-trimethylpentane RC ($TMP^{+\bullet}$). The dihedral angles φ characterizing the rotations in $DMB^{+\bullet}$ and $TMP^{+\bullet}$ are denoted in Figure 1a,b, respectively. The types of stationary PES points found were assigned by the normal vibrations analysis.

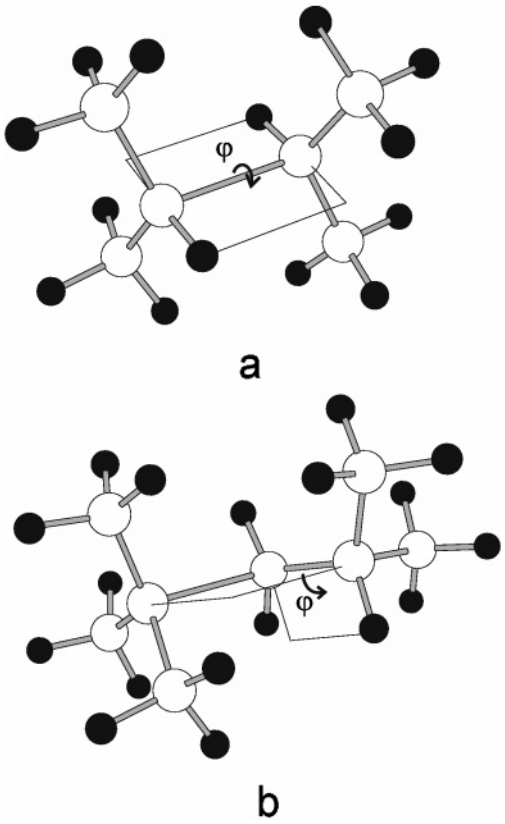

Figure 1. Energy favorable conformations of DMB (a) and TMP (b) radical cations. The rotation around C−C bonds shown by arrows leads to transition from one stationary point to another of the ground electronic state's PES (see the text).

Dependences of the energies of $DMB^{+\bullet}$ and $TMP^{+\bullet}$ species on the value of φ are shown in Figure 2a,b, respectively. The total energy values (E_{tot}) as well as relative ones (E_{rel}) calculated for the stationary structures of $DMB^{+\bullet}$ and $TMP^{+\bullet}$ are summarized in Tables 1 and 2, respectively. In all conformations of the RCs discussed, the unpaired electron is mainly located on the C_2-C_3 bond, which is in agreement with the data available in the literature.[1] The length of this bond for various conformations is within the range 2.0−2.3 Å for the $DMB^{+\bullet}$ and somewhat less for the $TMP^{+\bullet}$.

In the case of $DMB^{+\bullet}$, taking into account the correction for the zero-point vibrations energy (ZPE), we get two substantially different conformations that correspond to the local minima of PES and differ in the angle of rotation about the central C_2-C_3 bond. Angles of $\varphi \approx \pm 60°$ correspond to reflection symmetrical conformations. Interestingly, after the correction for ZPE the transition state at $\varphi = 180°$ transformed to the lowest in energy PES minimum for $DMB^{+\bullet}$. Figure 1a presents the conformation, which corresponds to $\varphi = 180°$.

For $TMP^{+\bullet}$, we also have the pair of equivalent in energy reflection symmetrical conformations, which correspond to the local PES minima at $\varphi \approx \pm 60°$. Similarly to the case of DMB, after the correction for ZPE the local PES minimum for $TMP^{+\bullet}$ shifted from 174° to 180°. Figure 1b shows one of the two lower in energy conformation of $TMP^{+\bullet}$ ($\varphi = 60°$). Within the same approach, the optimized geometry of neutral molecules of TMP

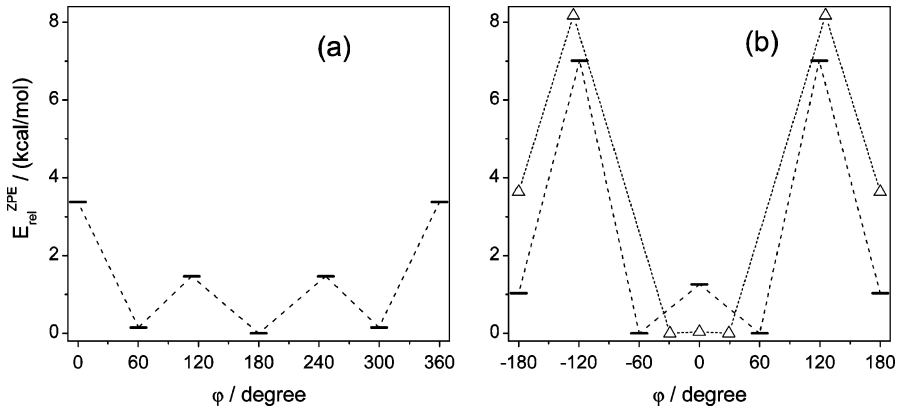

Figure 2. Energy profile of internal rotation in DMB (a) and TMP (b) radical cations according to the data obtained by the UB3LYP/6-31G* method taking into account corrections for ZPE. The angle φ of rotation around C−C bond involved is measured as shown in Figure 1. In part b the energies of stationary points of the rotation profile for TMP neutral molecule as calculated within the same approach are shown as triangles (Δ).

TABLE 1: Characteristics of the Stationary PES Structures and HFC Constants (*a*, mT) with Protons As Calculated for the 2,3-Dimethylbutane Radical Cation along the Internal Rotation Coordinate φ[a]

φ, deg	R,[b] Å	E_{tot}, au	PES point[c]	E_{rel}, kcal/mol	E_{rel}^{ZPE},[d] kcal/mol	a_H,[e] mT	a_{Me},[f] mT
0.0	2.286	−236.559803	TS	3.64	3.38 (TS)	0.00_5	1.46
±60.4	2.008	−236.565605	min	0	0.15 (min)	0.22_5	1.56; 1.62
±113.3	2.205	−236.563319	TS	1.43	1.47 (TS)	0.03	1.48; 1.62
±162.5	2.138	−236.564581	min	0.64	0.34 (−)	0.40_5	1.55; 1.56
±180.0	2.148	−236.563625	TS	1.24	0 (min)	0.47	1.55

[a] The dihedral angle of the rotation about the central C_2-C_3 bond (see Figure 1). [b] The length of the central C_2-C_3 bond. [c] As determined by the normal vibration analysis. Note that corrections for ZPE change the $DMB^{+\bullet}$ PES shape. [d] The relative energy corrected for ZPE. [e] HFC constant with α-protons. [f] HFC constant with β-protons averaged over the CH_3 protons by group's rotation.

TABLE 2: Characteristics of the Stationary PES Structures and HFC Constants (*a*, mT) with Protons As Calculated for the 2,2,4-Trimethylpentane Radical Cation along the Internal Rotation Coordinate φ[a]

φ, deg	R,[b] Å	E_{tot}, au	PES point[c]	E_{rel}, kcal/mol	E_{rel}^{ZPE},[d] kcal/mol	a_H,[e] mT	a_{CH_2},[f] mT	a_{t-Bu},[g] mT	a_{Me},[h] mT
0.0	2.120	−315.131951	TS	2.20_5	1.26 (TS)	3.31	−0.37	1.30	0.12
±60.0	2.070	−315.135465	min	0	0 (min)	0.43	−0.11; 0.10	1.34	0.07; 0.45_5
±119.3	2.253	−315.124269	TS	7.03	7.01 (TS)	1.31	−0.40	1.23_5	−0.03; 0.14
±174.2	2.066	−315.132758	min	1.70	1.39 (−)	6.95_5	−0.02; 0.25	1.37	0.20; 0.25_5
180.0	2.041	−315.131883	TS	2.25	1.03 (min)	7.21	0.19; 0.23	1.84	0.25

[a] The dihedral angle of the rotation about the C_3-C_4 bond (see Figure 1). [b] The length of the C_2-C_3 bond. [c] As determined by the normal vibration analysis. [d] The relative energy corrected for ZPE. [e] Proton of CH group. [f] Protons of CH_2 group. [g] Protons of *tert*-butyl group averaged over the *tert*-butyl and all of methyl groups rotation. [h] Protons of two methyl groups averaged over their rotation.

was calculated also and local minima of PES along the rotation around the C_3-C_4 bond for the molecule were found. The calculations predict these minima to correspond to φ angles of about ±30° and 180°. The energies of these minima as well as those of the transition states are presented in Figure 2b also. Note that the positions of PES extremes are shifted insignificantly along of the rotation coordinate while going from neutral TMP to $TMP^{+\bullet}$. At the same time, the energy of the minimum at $\varphi = 180°$ as well as of the transition state at $\varphi = 0°$ is significantly changed. For the purposes of this work it is important that the minimum energy at $\varphi = 180°$ is higher in neutral TMP molecule as compared to that of RC by about 3.6 kcal/mol. It results in low (<1%) abundance of $TMP^{+\bullet}$ in conformations corresponding to $\varphi = 180°$ at early nanoseconds because these appear due to vertical ionization of TMP molecules, which are in thermodynamic equilibrium.

HFC Constants. In solution, radical cations of studied alkanes can exist in various conformations with transition between them. These transitions are to lead to the modulation and the averaging of HFC constants that affect the spin dynamics in the radical pair.

To estimate the averaged values of HFC constants we have calculated energies as well as the HFC constants with protons that correspond for each stationary conformations of the ground electronic state of the studied RCs. Estimating HFC constants for stationary conformations, we suggested that the rotation of both methyl and *tert*-butyl groups was very fast. A typical value of the activation energy of methyl group rotation in hydrocarbons is 2−3 kcal/mol,[22] and their rotation in RCs at room temperature is sure to be fast enough to average HFC constants with the methyl protons. The same is likely to hold for the rotation of *tert*-butyl groups in which all nine protons can appear in equivalent positions. This assumption is supported by the fact that in hexamethylethane RC all the 18 protons are equivalent at room temperature.[10,13]

Additionally, these methyl and *tert*-butyl groups rotations were assumed to be incapable to rearrange noticeably the spin density and HFC constants in other fragments. Indeed, our calculations for *tert*-butyl group rotation, starting from the $TMP^{+\bullet}$ conformation shown in Figure 1b, gave the value of the energy barrier for the rotation as large as 1.9 kcal/mol and displayed a minor modulation of HFC constants with protons.

In the case of $DMB^{+\bullet}$, the averaging of HFC constants in each methyl group by their rotation and using the symmetry of RC allowed us to discriminate two groups of 6 methyl protons in each group and the group of 2 CH-protons. HFC constants calculated for the stationary structures of $DMB^{+\bullet}$ are summarized in Table 1.

TABLE 3: Parameters for Modeling of the Experimental Time-Resolved Magnetic Field Effect Curves Presented in Figures 3 and 4 as Well as the Averaged Calculated Values of HFC Constants (*a*, mT) with Protons in RCs

radical cation	parameters[a]	averaged values of HFC constants obtained by DFT calculations, mT
2,3-dimethylbutane	a(12H) = 1.6 mT; a(2H) = 0.64 mT $\Delta g \approx 7 \times 10^{-4}$ $T_2 = T_0 = 25$ ns; $T_1 = 2000$ ns	a(12H) = 1.56 a(2H) = 0.36
tetramethylethylene	a(12H) = 1.67 mT; $\Delta g \approx 2 \times 10^{-4}$ [b] $T_2 = T_0 = 17$ ns; $T_1 = 2000$ ns	a(12H) ≈ 1.67[b]
2,2,4-trimethylpentane	a(10H) = 1.3 mT; a(6H) = 0.37 mT $\Delta g \approx 9 \times 10^{-4}$ $T_2 = T_0 = 60$ ns; $T_1 = 2000$ ns	a(9H) = 1.34; a(6H) = 0.25 a(1H) = 0.59; a(2H) = −0.03
2,4,4- trimethylpentene-2	a(6H) = 1.65 mT; a(1H) = −0.83 mT $\Delta g \approx 1 \times 10^{-4}$ [b] $T_2 = T_0 = 22$ ns; $T_1 = 2000$ ns	a(3H) = 1.56; a(3H) = 1.8 a(1H) = −1.1; a(9H) = 0.1

[a] The *g*-value shift relative to *p*TP radical anion (2.0027[24]). [b] Experimental value determined by the OD ESR method.

As for $TMP^{+\bullet}$, we could distinguish several different magnetically equivalent proton groups after the averaging by methyl and *tert*-butyl fragments rotation. Table 2 shows HFC constants with the protons of these groups at stationary points of PES. It is worth noting that transitions between these conformations change most strongly the HFC constant for the CH proton.

In the next stage, we averaged the calculated values from Tables 2 and 3 over the stationary conformations by assuming that the statistical weight of accessible RC conformations with the relative energy E_{rel} (see Tables 1 and 2) is determined by the Boltzman factor $\exp(-E_{rel}/kT)$. The second assumption was that the transitions between such conformations occur rapidly enough to provide the fast spectral exchange between the corresponding lines of the radical ESR spectra. Recently, this approach was successfully applied to the HFC averaging in radical anions of fluorobenzenes.[23]

In the case of $DMB^{+\bullet}$, where all PES local minima are separated by comparatively low-energy barriers, all the stationary conformations are considered as accessible. After the complete averaging of HFC constants, the protons constitute two groups from 12 equivalent protons of methyl groups and from 2 protons of CH groups. The averaged HFC constants with the aforementioned protons are summarized in Table 3.

For the $TMP^{+\bullet}$, the averaging of HFC constants over conformations was carried out by assuming that fast exchange occurred only between conformations corresponding to angles φ of about 60° and 300° that were separated by the energy barrier of about 2 kcal/mol. The less favorable conformation ($\varphi = 180°$) separated by the energy barrier of 7 kcal/mol was not taken into account. The resulting estimated average HFC constants in $TMP^{+\bullet}$ are presented in Table 3.

The latter approximation is supported by the above-mentioned results of the calculations of local PES minima for TMP molecule whose conformational distribution is likely to determine an initial conformational distribution of $TMP^{+\bullet}$ immediately after electron transfer. According to these, the probability to find the molecule in the conformation corresponding to $\varphi = 180°$ is very low. Additionally, for the typical frequency 3×10^{12} s^{-1} for isopropyl fragment vibration along the rotational coordinate at $\varphi \sim 60°$ this energy barrier height results in a rather low rate of the transitions to the conformation at $\varphi = 180°$ ($<2 \times 10^7$ s^{-1}). Thus, within the time range studied the presence of this conformation of the $TMP^{+\bullet}$ can be neglected.

V. Experimental Results and Their Discussion

In this work, to observe RCs of branched alkanes the same approach has been used that was applied earlier for studying RC of the series of normal alkanes and hexamethylethane.[13,16] *n*-Hexane whose ionization potential is higher than that of both DMB or TMP was employed as a solvent. The branched alkane under study was added to solutions in concentrations of 0.03−0.3 M to provide the fast (~1 ns) capture of *n*-hexane holes by the solute. The molecules of *p*-terphenyl-d_{14} (*p*TP) served as electron acceptor and luminophore. The concentration of *p*TP was rather low (3×10^{-5} M) to exclude the electron transfer from *p*TP to alkane radical cations within the time range studied. TR MFE curves observed in these conditions was determined by spin evolution in the spin-correlated pairs $(DMB^{+\bullet})/(pTP^{-\bullet})$ or $(TMP^{+\bullet})/(pTP^{-\bullet})$. The main contribution to this evolution was made by HFCs in the RC, because the HFC constants in the radical anion of the perdeuterated *p*-terphenyl were small.[15,24]

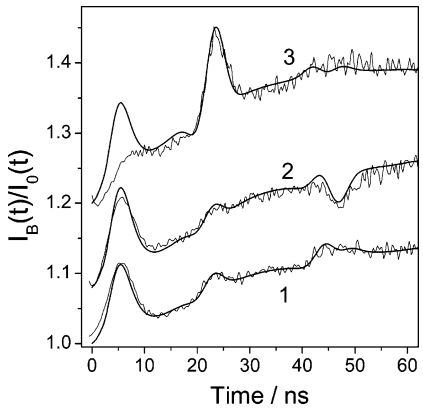

Figure 3. Experimental and calculated TR MFE curves for the solutions of 0.1 M DMB in *n*-hexane in magnetic fields of 0.1 T (curves 1) and 1.1 T (curves 2) as well as for 3 mM TME in cyclohexane in the magnetic field of 1.1 T (curves 3). The concentration of *p*TP was 3×10^{-5} M in all the cases. Modeling was performed using the parameters from Table 3.

DMB Radical Cation. Figure 3 shows the experimental and calculated curves of TR MFE for the 0.1 M DMB + 30 μM *p*TP solution in *n*-hexane at $B = 0.1$ T (curves 1) and $B = 1.1$ T (curves 2) at room temperature. Besides, the curves for the 3 mM tetramethylethylene (TME) + 30 μM *p*TP solution in cyclohexane at $B = 1.1$ T are presented (curves 3). This additional experiment with TME was performed because $TME^{+\bullet}$ was identified to be the product of unimolecular decay of $DMB^{+\bullet}$ in low-temperature freon matrices.[2,3] Cyclohexane was chosen as a solvent for TME to provide fast formation of $TME^{+\bullet}$ at comparatively low TME concentration. The higher rate constant of secondary radical cation $TME^{+\bullet}$ formation in cyclohexane ($\sim 3 \times 10^{11}$ M^{-1} s^{-1}) as compared to that in *n*-hexane was known to result from the high mobility of

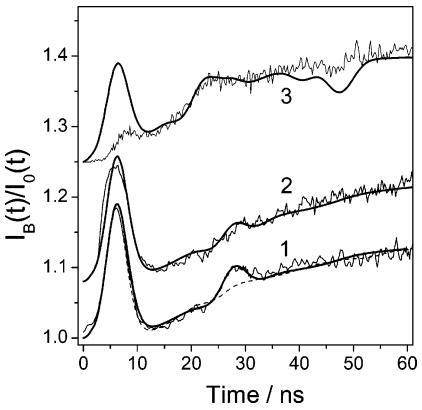

Figure 4. Experimental and calculated TR MFE curves for the solutions of 0.1 M TMP in *n*-hexane in the magnetic field of 0.1 T (curves 1) and 1.1 T (curves 2) as well as for 3 mM TMP2 in cyclohexane in the magnetic field of 1.1 T (curves 3). The concentration of *p*TP was 3×10^{-5} M in all the cases. Modeling was performed using the parameters from Table 3.

cyclohexane primary radical cations.[8,15] The decrease in TME concentration allowed us to diminish the complication of the spin dynamics due to the formation of dimeric species, $(TME)_2^{+\bullet}$.[15] It should be noted that in cyclohexane solutions the prompt luminescence is very strong at short times and insensitive to magnetic field. This luminescence effectively masks the first peak in the curve 3.

Table 3 summarizes the HFC constants of the $DMB^{+\bullet}$ and $TME^{+\bullet}$ as well as other parameters, which give the optimal modeling of the experimental TR MFE curves. Comparing experimental curves 1 and 3, we notice that the peculiarities of magnetic field effects in the DMB and TME solutions are observed at approximately the same moments of time. This indicates that for both $DMB^{+\bullet}$ and $TME^{+\bullet}$ the HFC constants for 12 equivalent methyl protons are very close. However, the radical cations forming in these two solutions differ in their *g*-factors. In the case of TME solutions, we have failed to observe any noticeable changes in the magnetic field effect with increasing magnetic induction from 0.1 to 1.1 T that indicates a minor difference in the *g*-factors of $TME^{+\bullet}$ and $pTP^{-\bullet}$. The *g*-value of $TME^{+\bullet}$ as determined using OD ESR measurement in squalane solution of TME amounts to 2.0029, which is actually close to that for $pTP^{-\bullet}$ (2.0027[24]).

On the contrary, as shown in Figure 3, for DMB solutions, the increase of the field causes substantial changes due to the shift of the *g*-value of $DMB^{+\bullet}$ as compared with the radical anion $pTP^{-\bullet}$. According to modeling, this shift amounts to 7×10^{-4}, which is similar to the shift measured earlier for the RC of another branched alkane, hexamethylethane.[13] It indicates that within the time range of 0−50 ns in the hexane solution of DMB, we observe a radical cation differing from $TME^{+\bullet}$. Besides, in this case, the magnetic field effect is well described by the RC model in which an unpaired electron interacts with groups of 12 and 2 equivalent protons with HFC constants close to the averaged values of $DMB^{+\bullet}$ calculated within DFT approach. We thus conclude that in our experiments, the radical cation of 2,3-dimethylbutane is observed.

TMP Radical Cation. Figure 4 shows the experimental and calculated curves of TR MFE for the TMP at magnetic induction $B = 0.1$ T (curves 1) and $B = 1.1$ T (curves 2), as well as ones at $B = 1.1$ T for 2,4,4-trimethylpentene-2 (TMP2, curves 3) solutions in *n*-hexane and cyclohexane, respectively. $TMP2^{+\bullet}$ seems to be a probable product of $TMP^{+\bullet}$ decay via splitting out the hydrogen molecule, as in the case of DMB.

As has been mentioned, after averaging over stationary structures, in $TMP^{+\bullet}$ we can discriminate several groups of protons with different HFC constants (Table 2). However, because the analytical formulas for TR MFE curves modeling are available only for two groups of equivalent protons, we have tried to find the two sets of HFC constants to describe the magnetic field effects observed for TMP solutions. According to calculations, the averaged value of HFC constant for two protons of the CH_2 group is very small and may be neglected in the modeling. As to the averaged HFC constant for CH proton, its value depends strongly on the contribution of conformation corresponding to $\varphi \approx 180°$ with the largest HFC constant. For calculated PES at room-temperature this contribution was not taken into account (vide supra) and the calculated value of the constant is not large, $a(CH) = 0.59$ mT (Table 3). Note, in the extreme case of free rotation its value gets much larger.

The good agreement between the calculated and the experimental curves for TMP solutions as presented in Figure 4 was achieved by assuming that the spin dynamics was determined by HFC with two groups of equivalent magnetic nuclei including 10 and 6 protons. This is possible if the averaged HFC constant for the proton of CH group is close to that of the protons of the *tert*-butyl fragment. If we assume that in $TMP^{+\bullet}$ the main contribution to HFC is made by two groups of either 9 and 7 or 9 and 6 equivalent protons, a satisfactory description of the experiment becomes impossible. Under these two suppositions, the curves that give the best description of the experiment are almost the same and are depicted by the dashed line in Figure 4. Importantly, only even numbers of equivalent protons with large HFC constant can result in a noticeable and positive peak,[15] as related to the slower buildup of the TR MFE curve background, at times about 30 ns. Therefore, the contribution of HFC with CH proton is likely to be higher than predicted by our estimations.

For $TMP2^{+\bullet}$, the magnetic field effect was modeled under the assumption that the main contribution to spin dynamics is made by six protons of two methyl groups, neglecting the difference in the HFC constants for these groups. In addition, account was taken of the interaction with the CH proton for which the HFC constant has a negative sign according to quantum-chemical calculations. Although in this case a good agreement between the calculated and experimental curves was not achieved, one can note that the values of the dominating HFC constants in $TMP2^{+\bullet}$, determining the location of the experimentally observed peculiarity (20−25 ns), are close to those obtained by B3LYP calculations (Table 3). Besides, we have observed also the OD ESR spectrum of $TMP2^{+\bullet}$, and this measurement also gave a close value for dominating the HFC constant ($a(6H) \approx 1.6$ mT, $g \approx 2.0029$). The modeling predicts one more peculiarity at 40−50 ns, which has not been found experimentally. However, the peculiarity at such a long time should be smoothed over by the small HFCs with the γ-protons of the *tert*-butyl fragment as well as due to nonequivalence of two methyl groups because of the absence of the rotation around the double bond. Table 3 summarizes parameters for which the curves in Figure 4 have been calculated.

Because of too many protons with different HFC constants in $TMP^{+\bullet}$, no peculiarities were observed in TR MFE curves in this case at times longer than 30 ns. This was why the shift of the *g*-value of $TMP^{+\bullet}$ relative to that of the *p*TP radical anion was obtained with lower accuracy as compared to the case of the DMB radical cation. Nevertheless, the observed *g*-value difference was typical for radical cations of branched alkanes.

Thus, having compared the experimental and model curves of the time-resolved magnetic field effect, we find that the RCs formed in the TMP and TMP2 solutions are quite different. Moreover, because the HFC constants obtained by both modeling the magnetic field effect curves for the TMP solution and calculating by the B3LYP method nearly coincide, it is concluded that in our experiments we observe the TMP radical cation.

Phase Relaxation and Lifetime of RCs. We varied the concentration of alkanes studied from 0.03 to 0.3 M and failed to reveal any changes in the magnetic field effect, which indicated the absence of degenerate electron exchange so as in the case of the hexamethylethane RC.[13] Thus, the observed phase relaxation for the studied RCs was not caused by electron exchange process.

The contribution of conformational transitions to the phase relaxation rate can be estimated using the well-known expressions of the Redfield theory[25]

$$\frac{1}{T_2} = (\gamma\Delta)^2\tau_c + \frac{1}{2T_1} \qquad \frac{1}{T_1} = \frac{2\gamma^2\Delta^2\tau_c}{1+(\gamma B\tau_c)^2} \qquad (6)$$

Here τ_c is the correlation time for the transitions, and Δ is a characteristic change in HFC constants upon that. For the energy barrier height of 3 kcal/mol and the frequency of torsional vibrations involved of about 10^{12} s^{-1}, one obtains $\tau_c \approx 10^{-10}$ s. Taking $\Delta \approx 1$ mT for $DMB^{+\bullet}$, we can get $T_2 \approx 300$ ns. Obviously, this mechanism does not contribute substantially to the observed relaxation and fails to have a substantial effect on the pattern of quantum beats over the time range of 50 ns where the main peculiarities of the magnetic field effect are observed.

In the case of $TMP^{+\bullet}$, fast transitions between conformations separated by low-energy barriers make also a small contribution to phase relaxation. However, transitions to the $\varphi \approx 180°$ conformation of $TMP^{+\bullet}$ with a large HFC constant should cause a drastic increase of singlet−triplet mixing similar to phase relaxation. If these transitions were the only reason for the phase relaxation, the latter should be strongly temperature dependent because the calculated activation barrier for the transition is rather high (about 7 kcal/mol). Experimentally, however, variations in the temperature of solution within 253−323 K cause no noticeable change in the values of parameter T_2 in the modeling.

Thus, it is reasonable to assume that the short times of phase relaxation (obtained with modeling) of studied alkane radical cations should be assigned not to the intramolecular modulation of HFC but to other processes. As rather probable ones, a monomolecular transformation of RC or the capture of positive charge by impurities with a lower ionization potential can be considered. Both of these processes result in a change in the ESR spectrum of a cation radical and the decay of the spin coherence in the radical ion pair. Reaction with impurities looks more plausible to be the reason because the rate of this process should depend on hexane viscosity that actually is changed only slightly with temperature within the range of 253−323 K. In any case the value of T_2 parameters for $DMB^{+\bullet}$ (about 20 ns) and $TMP^{+\bullet}$ (about 60 ns) obtained by modeling can be considered as the lowest estimate of the lifetime of these radical cations in processes other than the geminate ion recombination.

VI. Conclusions

For the first time, the radical cations of 2,3-dimethylbutane and 2,2,4-trimethylpentane in solution have been observed and identified by applying the method of time-resolved magnetic field effect. HFC constants with protons averaged by the fast rotation of methyl groups and conformation transitions in the radicals are determined. The constants obtained are close to those resulting from quantum-chemical DFT calculations. It has been demonstrated that at room temperature the lifetime of these radical cations in solution is, at least, several tens of nanoseconds.

Acknowledgment. The present work was financially supported by the Russian Foundation for Basic Research (grants 05-03-32620) and the program "Leading scientific schools" (NS-5078.2006.3)

References and Notes

(1) Toriyama, K. In *Radical Ionic Systems*; Lund, A., Shiotani, M., Eds.; Kluwer: Dordrecht, The Netherlands, 1991; pp 99−124.
(2) Saitake, Y.; Miyazaki, T.; Kuri, Z. *J. Phys. Chem.* **1973**, *77*, 2418−2420.
(3) Miyazaki, T.; Tsuruta, H.; Fujitani, Y.; Fueki, K. *J. Phys. Chem.* **1982**, *86*, 970−972.
(4) Tabata, M.; Lund, A. *Rad. Phys. Chem.* **1984**, *23*, 545−552.
(5) Ichikawa, T.; Shiotani, M.; Otha, N.; Katsumata, S. *J. Phys. Chem.* **1989**, *93*, 3826−3831.
(6) Mehnert, R. In *Radical Ionic Systems*; Lund, A.; Shiotani, M., Eds.; Kluwer: Dordrecht, The Netherlands, 1991; pp 231−284.
(7) Tagawa, S.; Hayashi, N.; Yoshida, Y.; Washio, M.; Tabata, Y. *Radiat. Phys. Chem.* **1989**, *34*, 503−511.
(8) Shkrob, I. A.; Sauer, M. C., Jr.; Trifunac, A. D. In *Radiation Chemistry: present status and future trends*; Jonah, C. D., Rao, B. S. M., Eds.; Elsevier: Amsterdam, The Netherlands, 2001; pp 175−221.
(9) Melekhov, V. I.; Anisimov, O. A.; Veselov, A. V.; Molin, Yu. N. *Chem. Phys. Lett.* **1988**, *148*, 429−434.
(10) Werst, D. W.; Bakker, M. G.; Trifunac, A. D. *J. Am. Chem. Soc.* **1990**, *112*, 40−50.
(11) Tadjikov, B. M.; Stass, D. V.; Molin, Yu. N. *J. Phys. Chem. A* **1997**, *101*, 377−383.
(12) Sviridenko, F. B.; Stass, D. V.; Molin, Yu. N. *Chem. Phys. Lett.* **1998**, *297*, 343−349.
(13) Bagryansky, V. A.; Borovkov, V. I.; Molin, Yu. N. *Phys. Chem. Chem. Phys.* **2004**, *6*, 924−928.
(14) Brocklehurst. B. *J. Chem. Soc. Faraday Trans.* **1997**, *93*, 1079−1087.
(15) Bagryansky, V. A.; Usov, O. M.; Borovkov, V. I.; Kobzeva, T. V.; Molin, Yu. N. *Chem. Phys.* **2000**, *255*, 237−245.
(16) Borovkov, V. I.; Gritsan, N. P.; Yeletskikh, I. V.; Bagryansky, V. A.; Molin, Y. N. *J. Phys. Chem. A* **2006**, *110*, 12752−12759.
(17) Anishchik, S. V.; Grigoryants, V. M.; Shebolaev, I. V.; Chernousov, Y. D.; Anisimov, O. A.; Molin, Yu. N. *Prib. Techn. Eksp. (Russ.)* **1989**, *4*, 74−79.
(18) Bagryansky, V. A.; Ivanov, K. L.; Borovkov, V. I.; Lukzen, N. N.; Molin, Yu. N. *J. Chem. Phys.* **2005**, *122*, 224503.
(19) Bagryansky V. A. *Dokl. Phys. Chem.* **2005**, *402*, Part 2, 105−108.
(20) Schulten, K.; Wolynes, P. G. *J. Chem. Phys.* **1978**, *68*, 3292−3297.
(21) Schmidt, M. W.; Baldridge, K. K.; Boatz, J. A.; Elbert, S. T.; Gordon, M. S.; Jensen, H.; Koseki, S.; Matsunaga, N.; Nguyen, K.; Su, S.; Windus, T. L.; Dupuis, M.; Montgomery, J. A. *J. Comput. Chem.* **1993**, *14*, 1347−1363.
(22) Kowalewski, J.; Liljefors, T. *Chem. Phys. Lett.* **1979**, *64*, 170−174.
(23) Barlukova, M. M.; Beregovaya, I. V.; Vysotsky, V. P.; Shchegoleva, L. N.; Bagryansky, V. A.; Molin, Yu. N. *J. Phys. Chem. A* **2005**, *109*, 4404−4409.
(24) Berndt, A.; Jones, M. T.; Lehnig, M.; Lunazzi, L.; Placucci, G.; Stegmann, H. B.; Ulmschneider, K. B. In *Numerical Data and Functional Relationship in Science and Technology*; Fisher, H., Hellwege, K.-H., Eds.; Landolt-Bornstein New Series, Group II, Vol. 9 part d1; Springer-Verlag: Berlin-Heidelberg-New York, 1980.
(25) Carrington, A.; McLachlan, A. D. *Introduction to magnetic resonance with application to chemistry and chemical physics*; Harper & Row: Publishers: New York, Evanston, London, 1967.